Electronic Supplementary Information (ESI)

for

Co-Containing Metal-Organic Framework for High-Performance Asymmetric Supercapacitor with Functionalized Reduced Graphene Oxide

Soumen Khan,[a,b] Sayan Halder,[a] Santanu Chand,[c] Anup Kumar Pradhan,[a] and Chanchal Chakraborty*,[a,b]

[a] Department of Chemistry, Birla Institute of Technology & Science (BITS) Pilani, Hyderabad Campus. Jawaharnagar, Samirpet, Hyderabad, Telangana 500078, India.

[b] Materials Center for Sustainable Energy & Environment (McSEE), Birla Institute of Technology and Science, Hyderabad Campus, Hyderabad 500078, India

[c]Department of Applied Chemistry, Graduate School of Engineering, The University of Tokyo, Bunkyo-ku, Tokyo 113-8656, Japan

*Corresponding Author: Chanchal Chakraborty

E-mail: chanchal@hyderabad.bits-pilani.ac.in

ORCID ID: https://orcid.org/0000-0002-4829-1367

Synthesis of MOF:

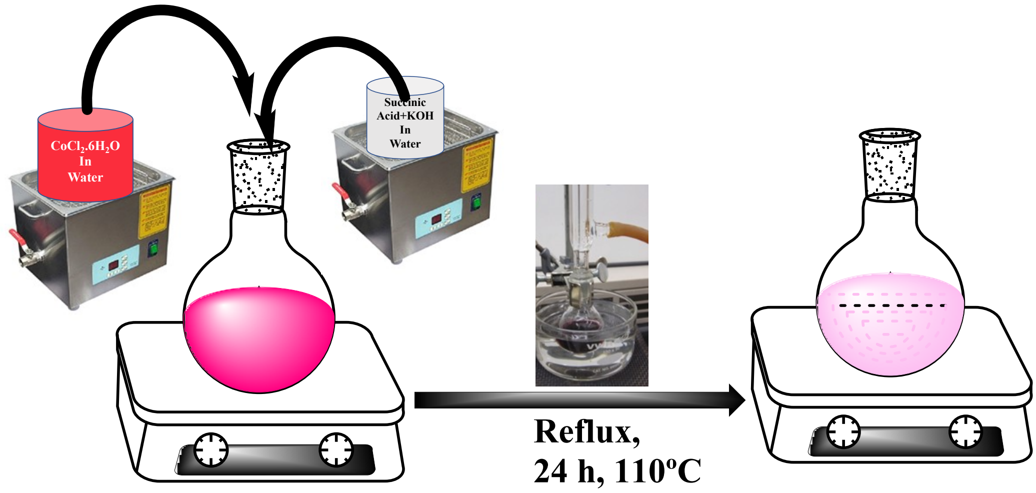

Scheme. S1 Synthesis of Co-MOF

At first, two 100 ml beaker were taken. 4 g (33.87 mmol) of succinic acid and 3.8 g (67.74 mmol) of KOH were taken in one of the beakers and added with 15 mL of water. The solution was sonicated for 15 min to dissolve the materials to form a completely clear solution. The solution was then transferred into a 100 mL round bottom flask. In another beaker, 8.33 g (35 mmol) cobalt chloride [$CoCl_2.6H_2O$] and 10 mL of water were taken, followed by a sonication of 15 min to make a clear salt solution. The solution was then added drop by drop into that round bottom flask containing the ligand in a stirring condition. After addition, the solution was refluxed at 110ºC for 24 hours to prepare the Co-MOF with a 92% yield.[1-3]

Reduction and functionalization of GO with PPD:

To synthesize covalently bonded multi-layered *p*-phenylenediamine (PPD) functionalized reduced graphene oxide, graphene oxide was synthesized first from natural graphite flake using the modified Hummer's method.[4]

To prepare PPD-rGO,[5] GO (60 mg) was dissolved and exfoliated in 120 mL of deionized water through ultrasonication. Subsequently, PPD (600 mg) and NH_3 solution (360 µL) were added. The mixture was refluxed under stirring conditions at 95 °C for 3 h and filtrated with Whatman

41 filter paper. The residue was rinsed in ethanol and poured into ultrasonication for 3 minutes. To remove the physically absorbed PPD, we repeated it at least five times. Finally, the residue was dried in an oven at 80 °C for 24 h.

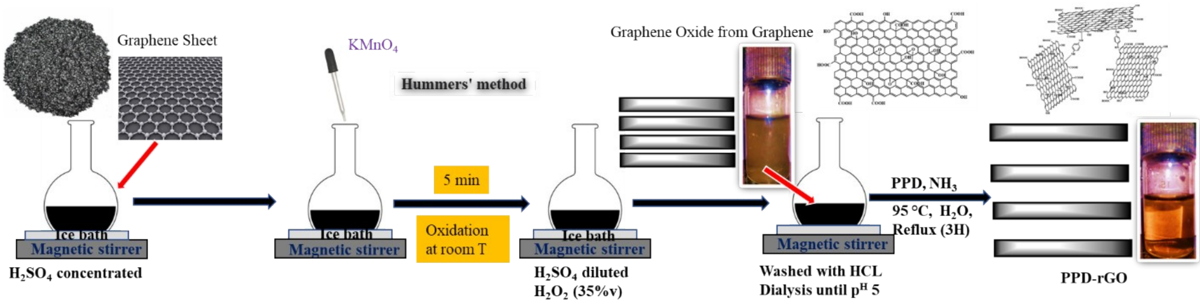

Scheme. S2 Synthesis of PPD-rGO from graphite flake.

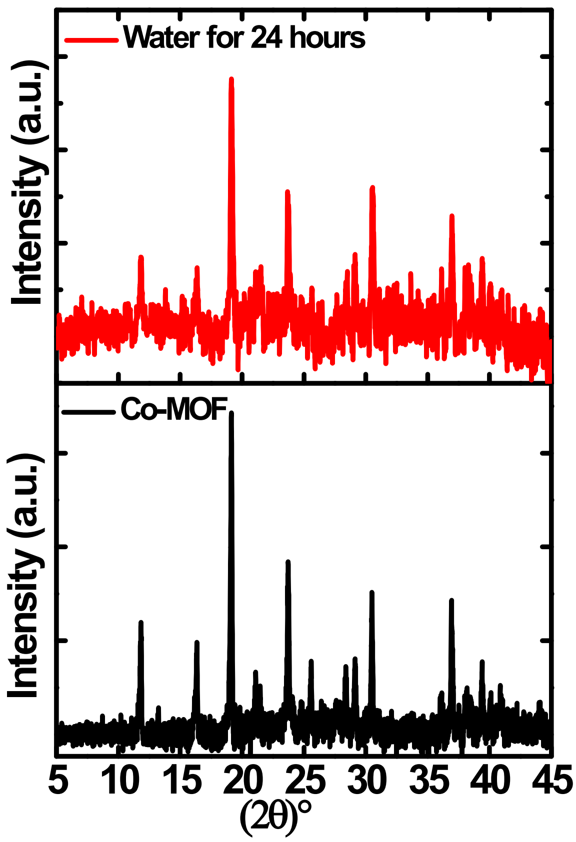

Fig. S1. Comparison of XRD pattern of Co-MOF and 24 hours water treated Co-MOF.

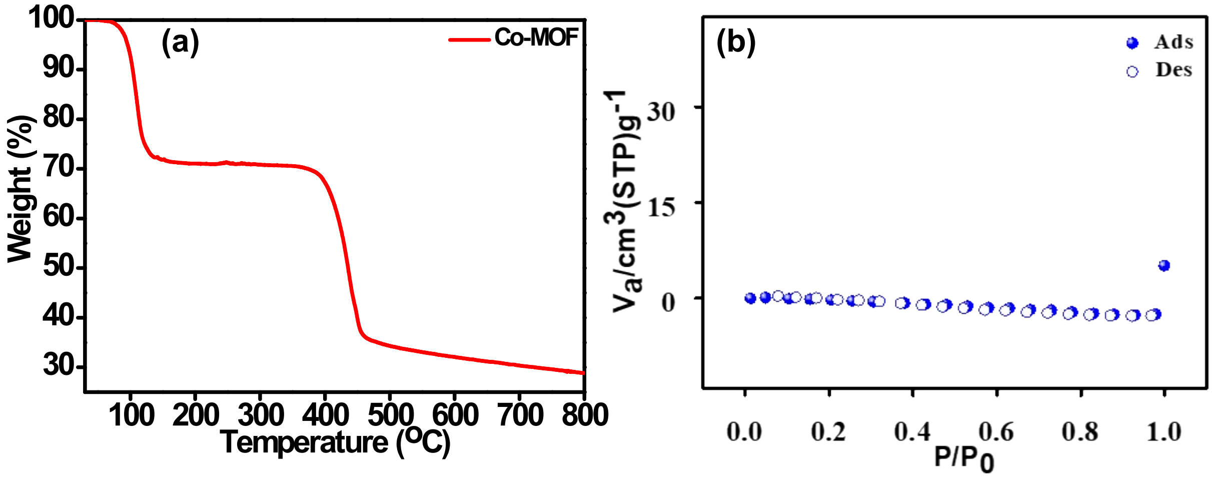

Fig. S2. (a) TGA curve of Co-MOF. (b) N_2 adsorption-desorption isotherm of Co-MOF.

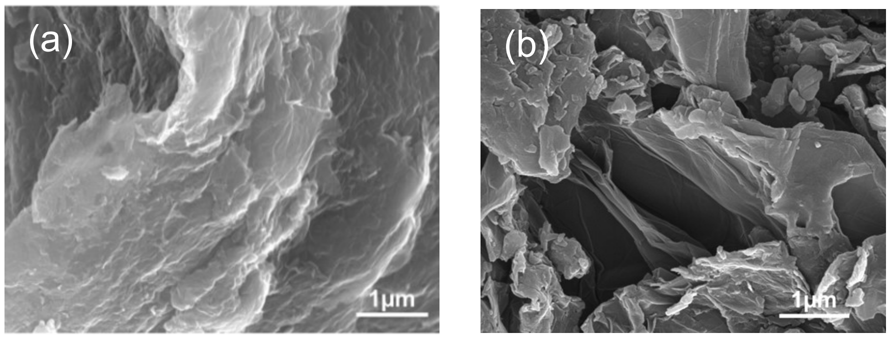

Fig. S3. The FESEM images of (a) GO and (b) PPD-rGO.

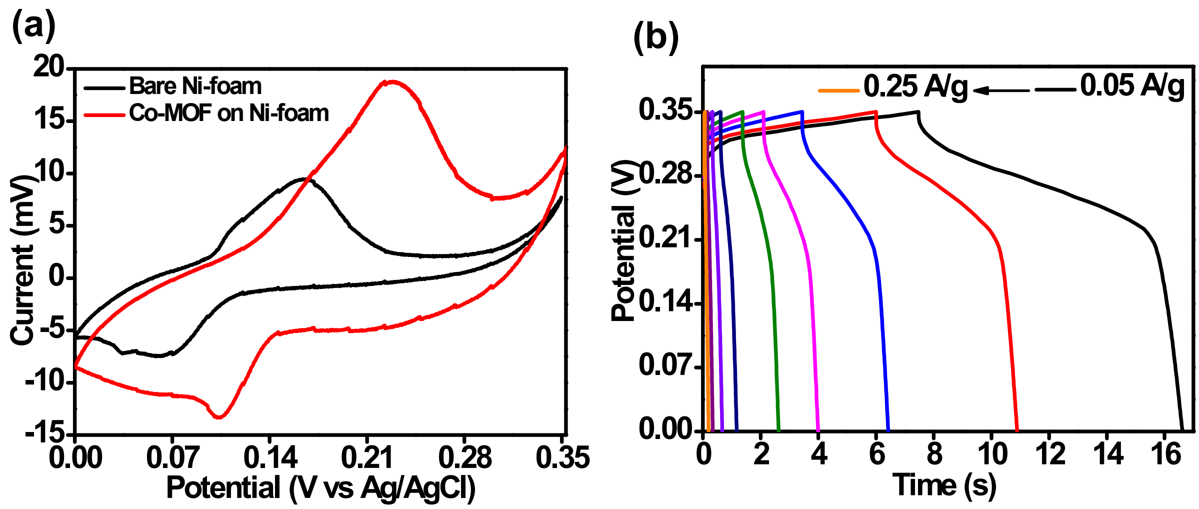

Fig. S4. (a) Comparison of the CV curves of bare Ni-foam and Co-MOF on nickel foam. (b) The GCD plots bare Ni-foam in a three-electrode system at a current density of 0.05 A/g to 0.25 A/g

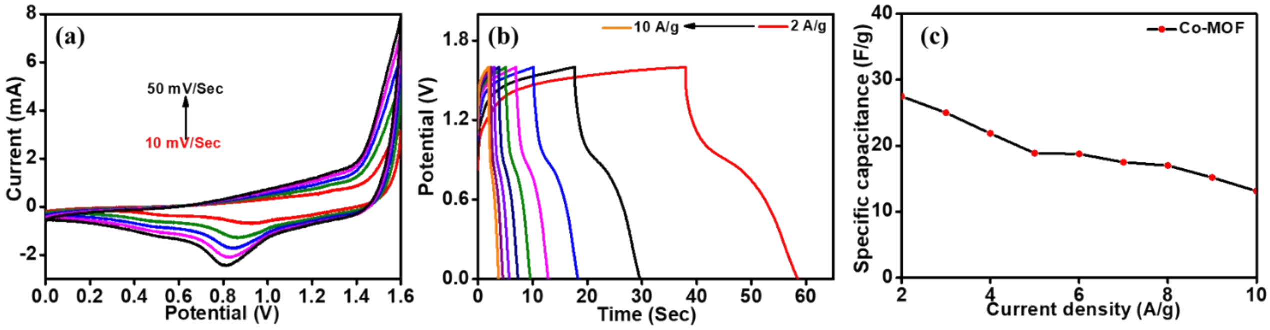

Fig. S5. Two electrode CV study of supercapacitor formed by Co-MOF with counter bare Ni-foam electrode: (a) CV curves at different scan rates at 10 mV/s to 50 mV/s; (b) GCD plot at a current density of 2 A g^{-1} to 10 A g^{-1}; (c) corresponding specific capacitance of the supercapacitor at different current density (2 A g^{-1} to 10 A g^{-1}) in the two-electrode system.

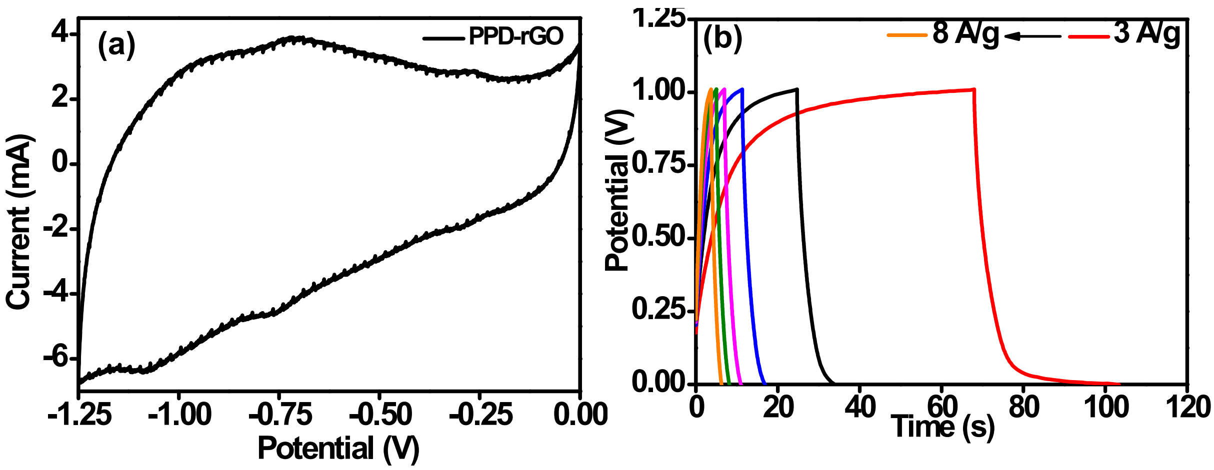

Fig. S6. (a) CV curve of PPD-rGO in the potential window of -1.25 V to 0 V. (b) GCD plot PPD-rGO in the current density range of 3-8 A/g in a three-electrode system.

Table S1. Comparison of the specific capacitance value of Co-MOF with other reported MOF-based electrodes.

Materials	**Potential window (V)**	**Electrolyte**	**Specific Capacitance (F g^{-1})**	**Current Density (A g^{-1})**	**Ref.**
MOF as electrode material					
3D Cd-MOF	−0.8 to 0.4 V	1 M NaOH/KOH/LiOH	647	4	[6]
Co-MOF with H_2tpa and dapz	0–0.5	2 M KOH	384	6	[7]
Zn-MOF	0-0.55		377	1	[8]
3D Co-MOF with ATA, bpdb	0-0.4	6 M KOH	325	5	[9]
3D Co-MOF-$CoMn_2O_4$	0-0.5	2 M KOH	1240	7	[10]
Co-MOF	**0-0.35**	**6 M KOH**	**425**	**2**	**This Work**
MOF@graphene					
Mo-MeIm derived MoO_3/RGO	0 - 0.8	PVA-H_2SO_4	617	1	[11]
Cu-MOF@rGO	−1-0.2	1 M Na_2SO_4	375	2	[12]
Cu-MOF/rGO (SD)	−0.5-0.7	1 M Na_2SO_4	685.33	1.6	[13]
rGO/HKUST-1	−0.1-1	0.5 M Na_2SO_4	385	1	[14]
Co-MOF-RGO	0 – 0.6	6 M KOH	430	1	[15]
Mn BTC derived Mn_3O_4/Graphene	-0.1 - 0.9	1 M Na_2SO_4	456	1	[16]
Co-MOF	**0-0.35**	**6 M KOH**	**425**	**2**	**This Work**

Table S2. Comparison of ED and PD of our ASC with other reports.

Materials	Counter Materials	ED ($Whkg^{-1}$)	PD ($kWkg^{-1}$)	References
3D Cd-MOF	Activated carbon (AC)	11.25	0.50	[6]
Co-Ni-MOF	AC	20.94	0.75	[17]
Co-MOF with H_2tpa and dapz	AC	24.13	4.42	[7]
Zn-MOF	AC	13.3	7.44	[8]
3D Co-MOF with ATA, bpdb	AC	50.03	2.31	[9]
Cu-atrz-BDC	rGO	9.96	0.00081	[18]
Ni-MOF-derived nickel phosphate	Ni-MOF-derived nickel phosphate	8	0.5	[19]
Ce-MOF/GO	Pt-wire	11.96	4.497	[20]
$Co(OH)_2$-Derived MOF	$Co(OH)_2$-Derived MOF	13.3	24.00	[21]
3D Co-MOF-$CoMn_2O_4$	AC	38.54	3.21	[10]
Co-MOF	**PPD-rGO**	**25.8 (max.)**	**11.9 (max.)**	**This Work**

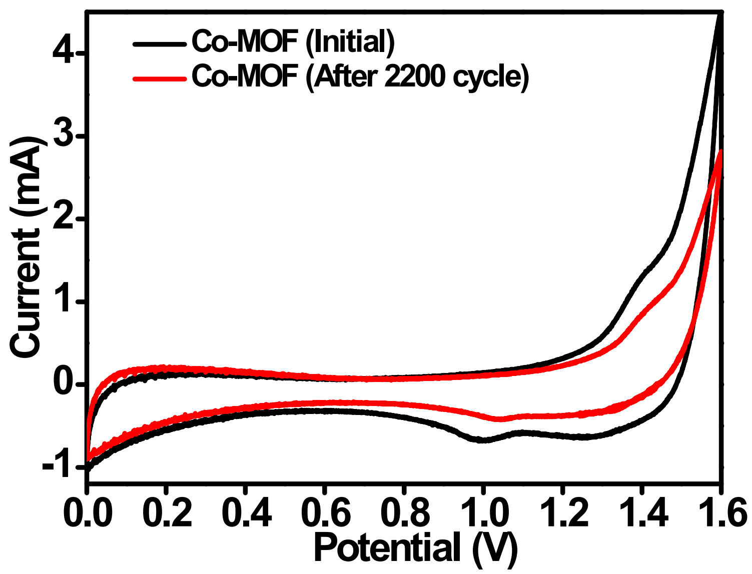

Fig. S7. CV curve after 2200 GCD cycle performance.

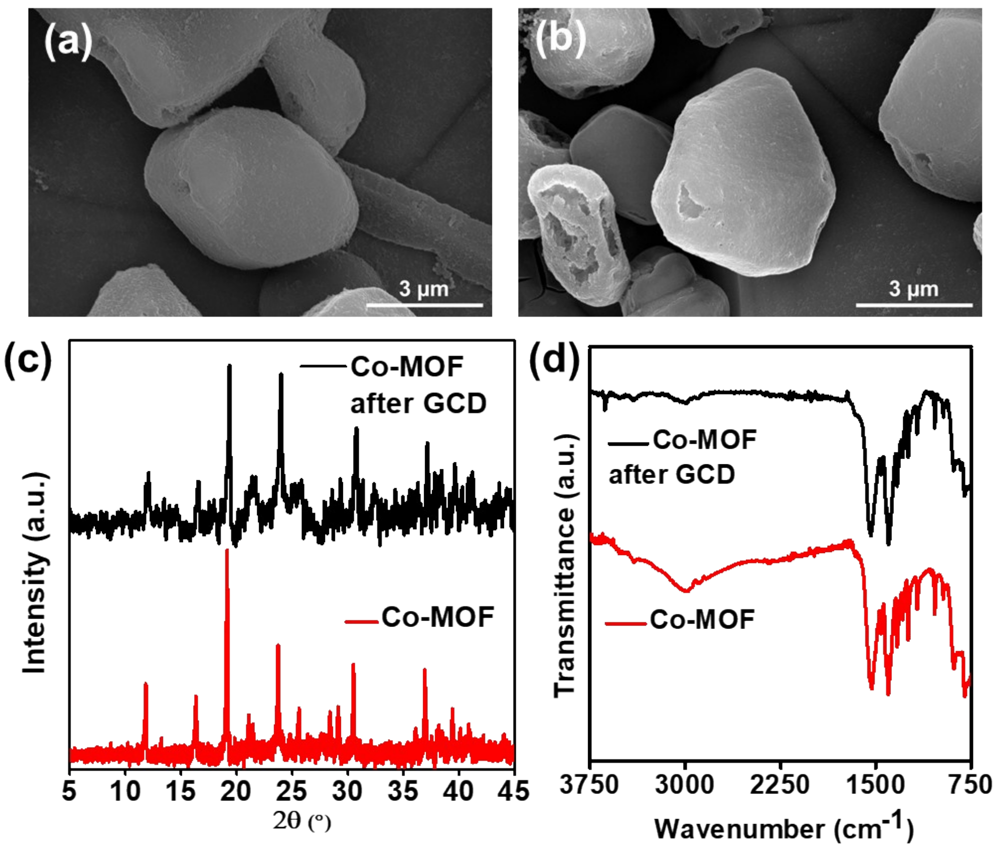

Fig. S8. The SEM images of Co-MOF (a) before and (b) after 2200 GCD cycles. The (c) PXRD and (d) FTIR study of Co-MOF before and after the GCD studies.

References

1. C. Livage, C. Egger, and G. Ferey, Hydrothermal versus nonhydrothermal synthesis for the preparation of organic− inorganic solids: the example of cobalt (II) succinate. *Chem. Mater.*, 2001, **13**, 410-414.
2. Z. H. Zhou, J. M. Yang, and H. L. Wan, Diamine substitution reactions of tetrahydrate succinato nickel, cobalt, and zinc coordination polymers. *Crystal Growth & Design.*, 2005, **5**, 1825-1830.
3. T. M. Li, J. H. Han, B. Q. Hu, F. Yu, and B. Li, A highly active oxygen evolution electrocatalyst derived from Co/Ni-succinic acid framework under mild conditions. *CrystEngComm*, 2022, **24**, 1453-1458.
4. B. Paulchamy, G. Arthi, and B. D. Lignesh, A simple approach to stepwise synthesis of graphene oxide nanomaterial. *J. Nanomed. Nanotechnol.*, 2015, **6**,1.
5. H. L. Ma, H. B. Zhang, Q. H. Hu, W. J. Li, Z. G. Jiang, Z. Z. Yu, and A. Dasari, Functionalization and reduction of graphene oxide with p-phenylene diamine for electrically conductive and thermally stable polystyrene composites. *ACS Appl. Mater. Interfaces.*, 2012, **4**, 1948-1953.
6. R. Deka, R. Rajak, V. Kumar, and S. M. Mobin, Effect of Electrolytic Cations on a 3D Cd-MOF for Supercapacitive Electrodes. *Inorg. Chem.*, 2023, **62**, 3084-3094.
7. S. Sanati, R. Abazar, A. Morsali, A. M. Kirillov, P. C. Junk, and J. Wang, An asymmetric supercapacitor based on a non-calcined 3D pillared cobalt (II) metal–organic framework with long cyclic stability. *Inorg. Chem.*, 2019, **58**, 16100-16111.
8. T. K. Ghosh, and G. R. Rao, Design and synthesis of mixed-ligand architectured Zn-based coordination polymers for energy storage. *Dalton Trans.*, 2023, **52**, 5943-5955.
9. R. Abazari, S. Sanati, A. Morsali, A. Slawin, and C. L. Carpenter-Warren, Dual-purpose 3D pillared metal–organic framework with excellent properties for catalysis of

oxidative desulfurization and energy storage in asymmetric supercapacitor. *ACS Appl. Mater. Interfaces.*, 2019, **11**, 14759-14773.

10. R. Abazari, S. Sanati, A. Morsali, and D. P. Dubal, High specific capacitance of a 3D-metal–organic framework-confined growth in CoMn 2 O 4 nanostars as advanced supercapacitor electrode materials. *J. Mater. Chem.*, 2021, **9**, 11001-11012.
11. X. Cao, B. Zheng, W. Shi, J. Yang, Z. Fan, Z. Luo, X. Rui, B. Chen, Q. Yan, H. Zhang, Reduced Graphene Oxide-Wrapped MoO_3 Composites Prepared by Using Metal–Organic Frameworks as Precursor for All-Solid-State Flexible Supercapacitors, *Adv. Mater.*, 2015, **27**, 4695-4701.
12. A.K. Gupta, M. Saraf, P.K. Bharadwaj, S.M. Mobin, Dual Functionalized CuMOF-Based Composite for High-Performance Supercapacitors, *Inorg. Chem.*, 2019, **58**, 9844-9854.
13. M. Saraf, R. Rajak, S.M. Mobin, A fascinating multitasking Cu-MOF/rGO hybrid for high performance supercapacitors and highly sensitive and selective electrochemical nitrite sensors, *J. Mater. Chem. A*, 2016, **4**, 16432-16445.
14. P. Srimuk, S. Luanwuthi, A. Krittayavathananon, M. Sawangphruk, Solid-type supercapacitor of reduced graphene oxide-metal organic framework composite coated on carbon fiber paper, *Electrochim. Acta*, 2015, **157**, 69-77.
15. M.S. Rahmanifar, H. Hesari, A. Noori, M.Y. Masoomi, A. Morsali, M.F. Mousavi, A dual Ni/Co-MOF-reduced graphene oxide nanocomposite as a high performance supercapacitor electrode material, *Electrochim. Acta*, 2018, **275**, 76-86.
16. K. Zhao, K. Lyu, S. Liu, Q. Gan, Z. He, Z. Zhou, Ordered porous Mn_3O4@N-doped carbon/graphene hybrids derived from metal–organic frameworks for supercapacitor electrodes, *J. Mater. Sci.*, 2017, **52**, 446-457.

17. *Inorg. Chem.*, 2019, **58**, 16100-16111J. Sun, X. Yu, S. Zhao, H. Chen, K. Tao, and L. Han, Solvent-Controlled Morphology of Amino-Functionalized Bimetal Metal–Organic Frameworks for Asymmetric Supercapacitors. *Inorg. Chem.*, 2020, **59**, 11385-11395.

18. Ma, Y., Gao, G., Su, H., Rong, H., Lai, L. and Liu, Q., A Cu 4 cluster-based MOF as a supercapacitor electrode material with ultrahigh capacitance. *Ionics*, 2021, **27**,1699-1707.

19. R. Bendi, V. Kumar, V. Bhavanasi, K. Parida and P. S. Lee, Metal organic framework-derived metal phosphates as electrode materials for supercapacitors. *Adv. Energy Mater.*, 2016, **6**, 1501833.

20. R. Ramachandran, W. Xuan, C. Zhao, X. Leng, D. Sun, D. Luo, and F. Wang, Enhanced electrochemical properties of cerium metal–organic framework based composite electrodes for high-performance supercapacitor application. *RSC Adv.*, 2018, **8**, 3462-3469.

21. T. Deng, Y. Lu, W. Zhang, M. Sui, X. Shi, D. Wang, and W. Zheng, Inverted Design for High-Performance Supercapacitor Via Co (OH) 2-Derived Highly Oriented MOF Electrodes. *Adv. Energy Mater.*, 2018, **8**, 1702294.